

Supporting information

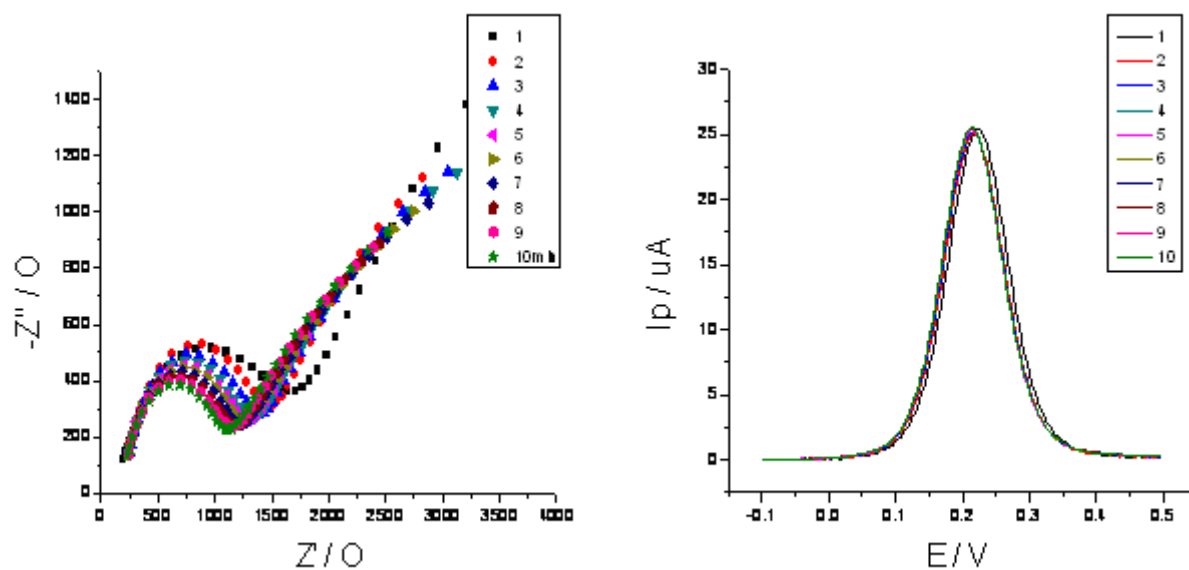


FIGURE S1: Nyquist diagrams of electrochemical impedance spectra and DPV diagrams of BGC823/PDMS-PDDA/Au in continuous detection for 10 times in homogeneous solution.

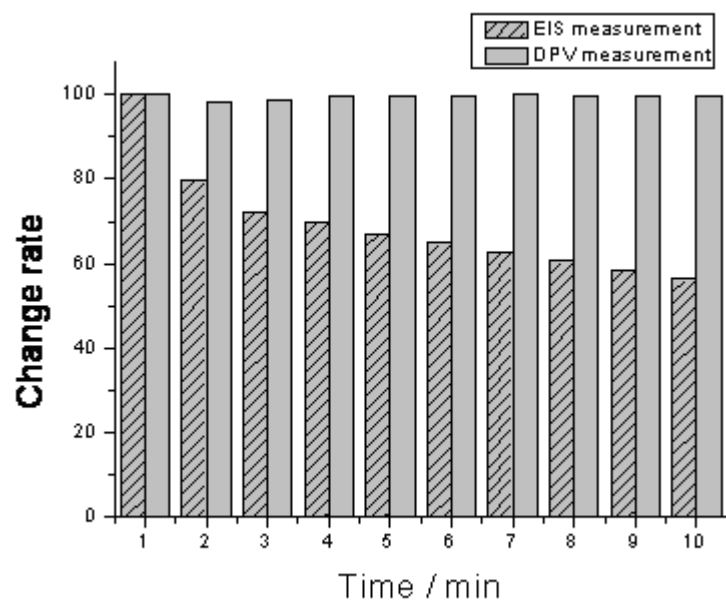


FIGURE S2: Change rates of resistance and peak current by each measurement in detection of 10 times.

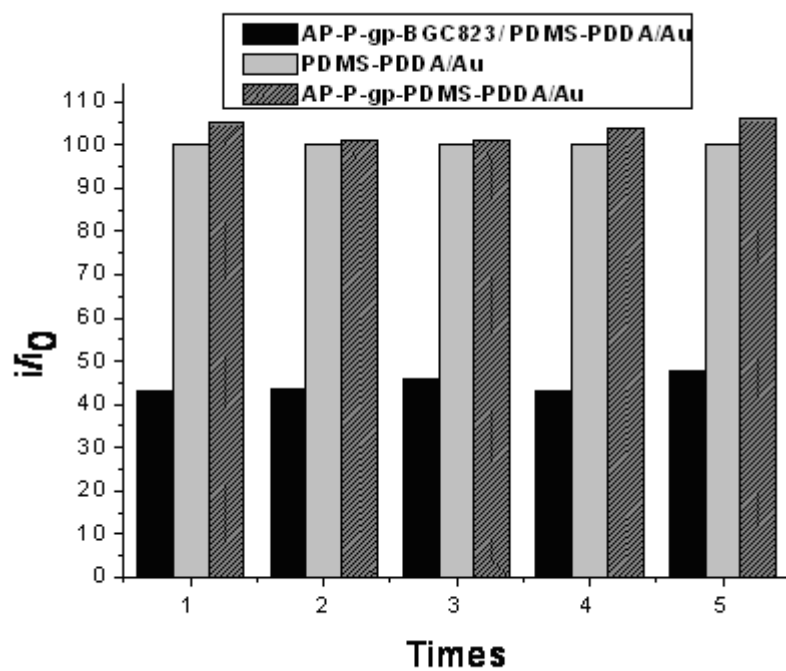


FIGURE S3: Ratios of peak currents of $[\text{Fe}(\text{CN})_6]^{3-}$ on AP-P-gp-BGC823/PDMS-PDDA/Au or AP-P-gp-PDMS-PDDA/Au to that on PDMS-PDDA/Au. (i_0 : the peak current of $[\text{Fe}(\text{CN})_6]^{3-}$ on PDMS-PDDA/Au)

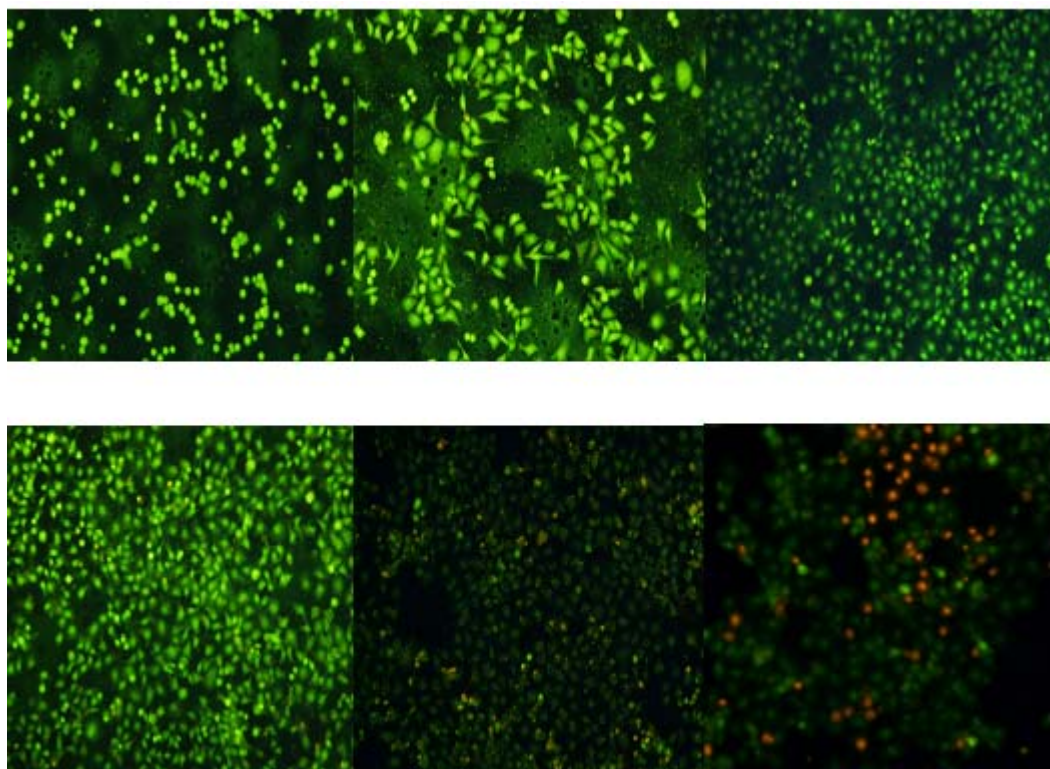


FIGURE S4: Fluorescent images ($856.8\ \mu\text{m} \times 644.8\ \mu\text{m}$) of BGC823 cells cultivated on PDMS-PDDA modified Au slides at (a) 4 h, (b) 8 h, (c) 24 h, (d) 48 h, (e) 72 h, (f) 96 h. Staining with AO and EB: live cells (green), dead cells (red).

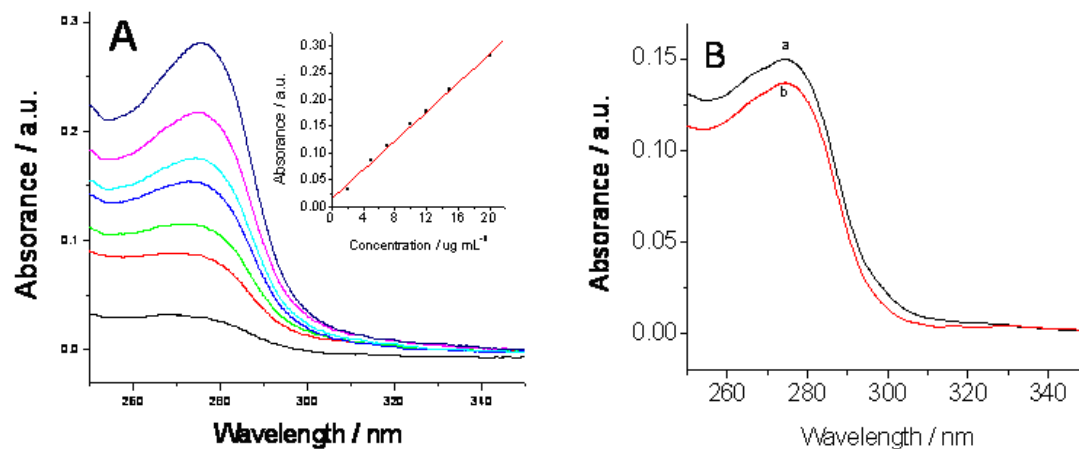


FIGURE S5: UV-visible absorption spectra of P-gp (A) dissolved in pH 7.4 PBS with concentrations increasing from 2.0-20 $\mu\text{g mL}^{-1}$ (from lower to upper), and P-gp (B) dissolved in pH 7.4 PBS after 1h incubation on the PDMS-PDDA film (a) and BGC823/PDMS-PDDA film (b), respectively. Inset A: Plot of P-gp concentration vs. peak absorbance at 276 nm.